EPR spectroscopic characteristics of quartz from tungsten-mineralized and tungsten-free quartz veins in Sewariya–Govindgarh area, Rajasthan, India

U. Dhanya[1], M. S. Pandian[1,*], C. Shiyamala[2], R. Sivasubramaniam[1], D. Ponraju[3] and P. Sambasiva Rao[2]

[1]Department of Earth Sciences and [2]Department of Chemistry, Pondicherry University, Pondicherry 605 014, India
[3]Radiological Safety Division, Indira Gandhi Centre for Atomic Research, Kalpakkam 603 102, India

The EPR spectra of quartz samples from tungsten-mineralized and tungsten-free quartz-rich veins of Sewariya–Govindgarh area, Rajasthan are examined to identify various types of point defects in quartz occurring in these two contrasting domains, and their significance in recognizing the affinity of quartz (i.e. tungsten-associated or tungsten-free). The EPR spectra of quartz occurring in these two environments show a clear distinction in the relative intensity of E_1' and peroxy centres after gamma irradiation of the samples. The results show that incidence of tungsten mineralization in a quartz vein can be recognized from EPR spectra of quartz.

Keywords: Crystal defects, EPR spectra, metal impurities, quartz veins, tungsten mineralization.

QUARTZ is one of the most abundant minerals found in the rocks of the earth crust and formed under a wide range of *P–T* conditions prevailing in the crust. In different crustal environments, quartz is crystallized from silicate melt, precipitated from aqueous solution or formed as a result of solid state transformation during metamorphic events. Ore deposits of metals like W, Li, Mo and Au, often occur in the form of veins that dominantly contain quartz. Such metalliferous quartz veins are known to have formed by precipitation from aqueous solutions, usually at temperatures of 200 to 550°C and 1 to 3 kb pressure, few kilometres below the surface[1].

Quartz is one of the purest natural minerals and is without structure defects, i.e. ideal crystal structure which does not contain unpaired electrons and thus shows no EPR signals. When foreign ions or atoms having unpaired electrons are present in the structure of quartz, each such ion or atom acts as a paramagnetic probe (by themselves or after irradiation) and produces characteristic resonance lines in the EPR spectra. Crystal defects like oxygen-hole (E_1' centre) in quartz are also paramagnetic and produce resonance lines in the EPR spectra. The impurities commonly found in quartz can be classified as substitutional (occupying the place of Si^{4+}) or interstitial (occupying vacant space in the large *c*-axis channels). Substitutional impurities are aluminum centres [Al^{3+}, with or without charge-compensating ions (M^+) such as Na^+, Li^+, H^+], germanium centres $[GeO_4/M^+]^0$, P^{4+}, Ti centres $[TiO_4/M^+]^0$, etc.[2–7]. The interstitial impurity is Fe^{3+}. Also, a few impurities such as $4H^+$ and $3H^+$ are known to substitute for Si^{4+}. Other defects are E_1' centre, peroxy radical (dry OHC and wet OHC), O_3' and oxygen vacancy[4,8].

Any system having at least one unpaired electron is EPR-active. The spin and orbital angular momenta of the electron interact with the applied magnetic field to give rise to various electron spin energy levels. Transitions between these energy levels, induced by radiofrequency, will give rise to an EPR spectrum. The EPR spectrum can be complicated if hyperfine (due to nuclear spin of the central metal atom), zero-field (due to the interaction between two unpaired electrons) and superhyperfine (due to nuclear spin of ligand atoms) effects are present. Generally, most of the inorganic and organic free radicals will have *g* values close to 2.0023 (free-electron *g* value)[9].

In the present study an attempt has been made to examine the differences in crystal defects and metal impurities in quartz from tungsten-bearing and tungsten-free hydrothermal quartz veins occurring in Sewariya–Govindgarh area, Rajasthan, India, using EPR spectroscopy.

Geological setting and description of samples

Sewariya–Govindgarh area lies along the western margin of South Delhi Fold Belt in the Aravalli craton, where metasediments and metavolcanics of Mesoproterozoic Barotiya Group (of the Delhi Supergroup) are intruded by an older biotite granite gneiss called Sewariya granite (SG) and a younger tourmaline leucogranite called Govindgarh granite (GG; Figure 1). The Geological Survey of India

*For correspondence. (e-mail: mspandian59@hotmail.com)

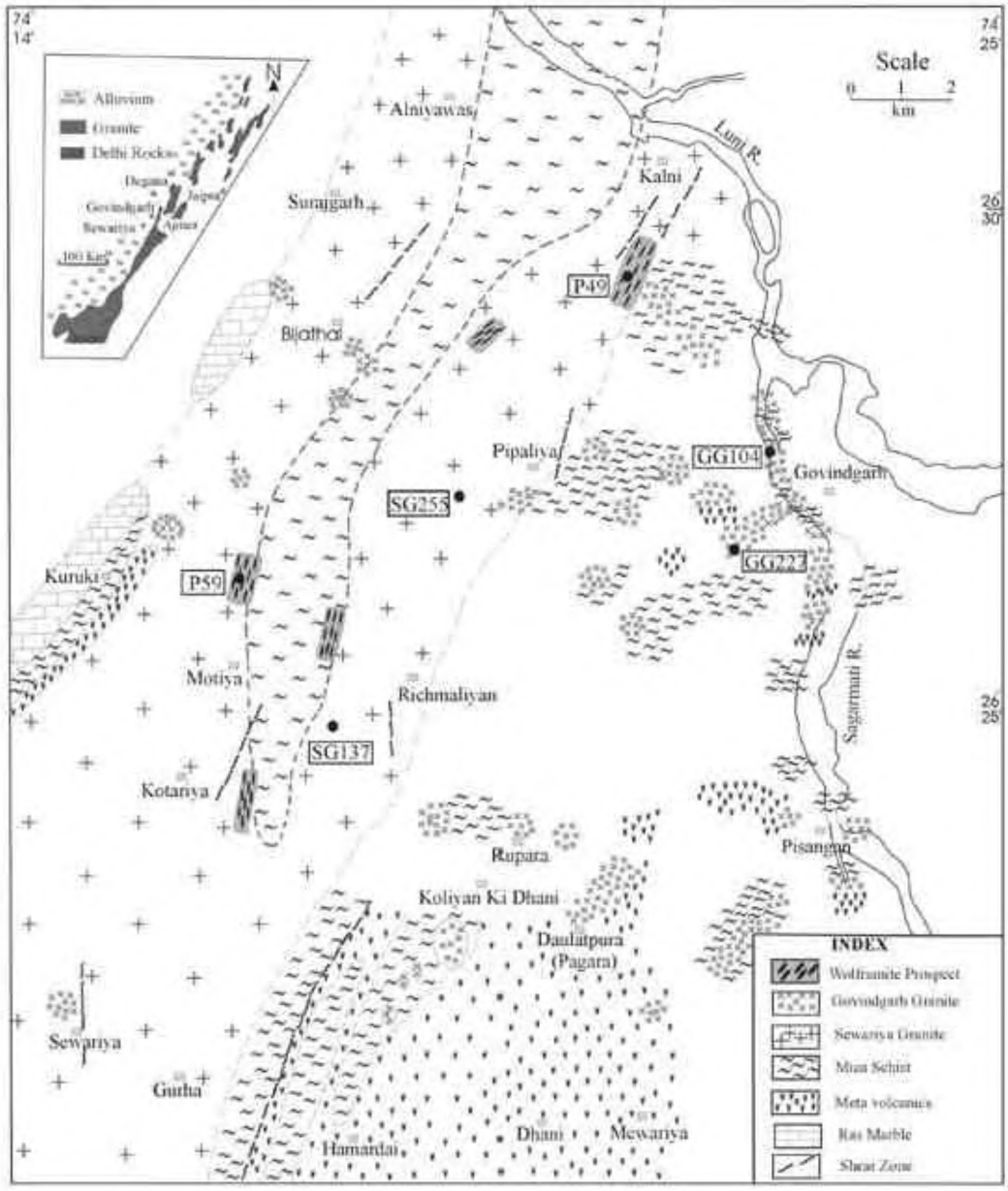

Figure 1. Geological map of Sewariya–Govindgarh area, Rajasthan, showing sample location (modified from Bhattacharjee *et al.*[11], and Pandian and Dutta[12]).

reported wolframite mineralization in quartz veins from Motiya, Pipaliya, Richmaliyan, Kotariya and Bijathal prospects[10,11], where these tungsten-mineralized quartz veins trending N–S to NNE–SSW occur along the sheared contact between Barotiya mica schist and Sewariya granite. Tungsten concentration[11] in these quartz veins ranges from 0.1 to as high as 3.5 wt%. These veins consist of milky-white quartz, tourmaline, muscovite and wolframite. On the basis of enrichment of tungsten in Govindgarh granite, and presence of colour-zoned tourmaline in Govindgarh granite and wolframite-bearing quartz veins, Pandian and Dutta[12] inferred that the tungsten-mineralized veins were formed during the hydrothermal stage of leucogranite magmatism.

Apart from the tungsten-mineralized quartz veins localized along sheared contact between mica schist and Sewariya granite, the two granites are also intruded by quartz veins at several locations away from the tungsten prospects. SG is intruded by grey-coloured quartz veins which do not contain wolframite. These quartz veins show evidence of brittle deformation with displacement of a few centimetres along a number of fault planes in different locations. A large number of these quartz veins is found near Kalni, and along Bhutiya Bala river section near Kotariya. These

quartz veins have been formed during late stage of magmatic event which produced SG.

GG is intruded by quartz–tourmaline veins which contain milky-white quartz, comparable with quartz veins of tungsten prospect; however, the presence of wolframite has not yet been recorded in these quartz veins occurring within GG. Unlike the grey quartz veins in SG, the milky-white quartz veins in GG are undeformed. They have formed during late stage of the magmatic activity which produced GG.

The samples for this study were collected from three different types of quartz veins occurring in the Sewariya–Govindgarh area, namely (i) quartz veins occurring within the older biotite granite (Sewariya granite), which are grey-coloured and free from tungsten mineralization; (ii) quartz veins occurring within the younger tourmaline leucogranite (GG), which are milky-white in colour and whose tungsten potential is not yet explored, and (iii) wolframite-bearing quartz veins occurring within mica schist in the well-explored Motiya and Pipaliya tungsten prospects. Two samples of quartz were collected from each type of these veins. Sample locations are given in Figure 1.

Experimental details

Samples of quartz were crushed to 100–300 μm size, washed with distilled water, allowed to dry and compound/other mineral grains were removed under stereoscopic microscope. One fraction of natural sample was used directly for EPR spectroscopy. Separate fractions (about 5 g) of each sample were subjected to the following treatments before obtaining the EPR spectra. (i) Heating at about 500°C for 20 min. This treatment was done to evaporate any volatiles present in the sample. (ii) Heating at about 800°C for 15 min. This was done to study the effect of crystallographic inversion of quartz. (iii) Leaching with 6N HCl for 30 min followed by leaching with 6N HNO_3 for 30 min to remove surface impurities like carbonates, sulphides, etc. (iv) In addition to previously mentioned acid treatment, leaching with 10% HF for 45 min to remove silicate impurities from the surface. Acid-leached samples were subsequently washed with distilled water and allowed to dry. In this way, at the first stage six-subsets (one natural and five treated) were prepared for each of the six quartz samples.

EPR spectra were obtained for all these samples at room temperature using JEOL JE-TES100 EPR spectrometer, at the Department of Chemistry, Pondicherry University under the following conditions: frequency ~ 9.4 GHz, power 1.0 mW, sweep time 2 min, time constant 0.03 s, magnetic field strength 400 ± 250 or 250 ± 250 or 336 ± 40 or 335 ± 5 mT, and amplitude 10 to 100.

In the second stage, one natural sample from each of the three types of quartz veins (SG-137, P-49 and GG-227) and their subsets which were subjected to the two types of acid treatments were taken for further experiment with gamma irradiation. Each of these samples was divided into five subsets (corresponding to five different dosage), and irradiated in the Gamma Chamber (^{60}Co source strength 304.9 curie and dosage 58 krads/h) at IGCAR, Kalpakkam for 1, 2, 4, 6 and 8 h. EPR spectra were obtained for these irradiated samples also at room temperature within 12 h after irradiation, under the same operating conditions as for the samples before irradiation.

Generally, irradiation of quartz samples with gamma rays produces paramagnetic centres, which give rise to broad EPR resonance lines. In order to obtain well-resolved spectra, these samples are cooled to low temperatures[4]. Hence, in order to confirm the creation of any extra radicals produced after irradiation, the EPR spectra for all the irradiated samples were also recorded at 77 K. However, in the present set of samples, we did not notice any additional radicals. The low-temperature measurements were carried out using a liquid nitrogen Dewar.

The g factor for various centres was calculated using the equation,

$$g = 71.44836 \times (\nu/B),$$

where ν is the microwave frequency in GHz and B is magnetic field strength in mT.

Results and conclusion

The g values of resonance lines which appeared in all samples scanned after the first stage of sample preparation discussed above, are listed in Table 1. The EPR spectra of three quartz samples (SG-137, P-49, GG-227) prepared in the first stage (before gamma irradiation), representing the three types of quartz veins are given in Figure 2. All the samples of quartz from the three different types of quartz veins, prior to gamma irradiation yielded a single strong resonance line in the magnetic field 335 ± 5 mT, whose g value is close to 2.002. The g factor of this resonance line in all these spectra corresponds to E_1' centre (oxygen hole). From the difference in intensity of this resonance line among various samples, it is observed that the number of E_1' radicals is less in tungsten-free quartz compared to tungsten-bearing quartz. This resonance line does not appear in the samples that were heated to about 800°C. Absence of this radical in quartz samples after high temperature treatment indicates its instability, a common factor for most radicals. All the paramagnetic impurities in quartz are known to convert back to their diamagnetic state after heating to high temperature[9]. The other resonances whose g value is different from 2.0 (see Table 1) occur from various other defect centres in quartz, arising from metal ions[4], which are not considered in the present study. Some of the samples show a resonance line whose g value is around 2.2, and this corresponds to Fe^{3+} impurities[4] in

Table 1. *g* values of resonance lines in EPR spectra of quartz samples

	g value				
	Subset of sample				
Sample no.	Natural	$HCl + HNO_3$ leached	$HCl + HNO_3$ + HF leached	Heated at 500°C	Heated at 800°C
SG-137	2.009 2.002	3.288* 2.009 2.002	3.430* 2.009 2.002	2.865* 2.002	2.842* 2.007
SG-255	2.381* 2.001	2.475* 2.009 2.002	2.008 2.001	2.978* 2.004 2.002	2.747* 2.012
P-49	2.714* 2.009 2.004	2.368* 2.009 2.001 2.000*	3.127* 2.009 2.002 2.000	2.436* 2.012 2.005	2.486* 1.998
P-59	2.002	2.009 2.002	2.672* 2.009 2.002	2.004 2.002	2.851*
GG-227	2.592* 2.015 2.009	2.010 2.002	2.010 2.002	2.413* 2.004 2.002	–
GG-104	2.677* 2.002	2.001	2.365* 2.193 2.002	2.834* 2.011 2.005	2.176*

*Broad unresolved peak. Not considered in the present work.

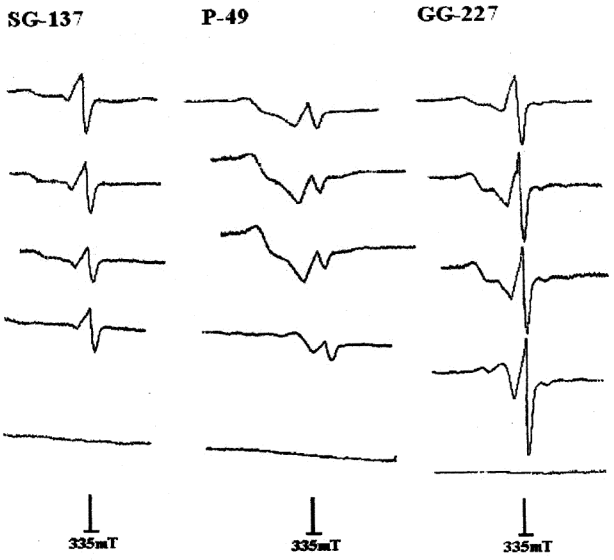

Figure 2. EPR spectra of three types of quartz samples before gamma irradiation. Five spectra from top to bottom in each column correspond to subset of each sample: natural, leached with $HCl + HNO_3$, leached with $HCl + HNO_3 + HF$, heated to 500°C, and heated to 800°C. Scan range = 335 ± 5 mT.

quartz. The spectra taken in the magnetic field 400 ± 250 and 250 ± 250 mT show broad lines in some samples, which correspond to unresolved and spin broadened lines from metal ions like Al and Ge[4].

From Figure 2 and Table 1, it is observed that subjecting the samples to two types of acid leaching and heating up to 500°C does not have any appreciable effect on the EPR spectra, except for a small reduction in the intensity of resonance lines compared to those of natural samples. This is due to partial loss of radicals, particularly after leaching with HF. This feature also confirms that the resonance lines are strictly due to structural defects in quartz and not related to any surface impurities.

The EPR spectra of three natural samples of quartz (SG-137, P-49, GG-227) prepared in the second stage (after gamma irradiation for 1, 2, 4, 6 and 8 h corresponding to the dosage of 58, 116, 232, 348 and 464 krad respectively) and representing the three types of quartz veins are given in Figure 3. In all the three subsets of the quartz samples irradiated for 1, 2, 4, 6 and 8 h in addition to the strong resonance line of the E_1' centre, another resonance line also appeared. The *g* value of the second resonance line shows that it is due to peroxy radical (OH centre)[9]. These two resonance lines (oxygen hole and OH centre) do not overlap, thus allowing us to measure the intensities accurately. As the widths of the two resonance lines are almost constant, their intensities (amplitudes) are a measure of concentration of the radicals. A comparison of the ratio of intensities of the two resonance lines in the EPR spectra as a function of irradiation time, shows contrasting trends in different types of quartz (Figure 4). As it is difficult to have

the same amount of sample in the EPR cavity during measurement of EPR spectra for various samples, we have considered the ratio of E_1' centre to another centre, which has almost the same intensity during irradiation dosage. Preliminary experiments have shown that the formation of peroxy radical is almost the same for different durations of irradiation. The reason may be that the first one hour of irradiation has produced sufficient amount of centres and has got saturated. Therefore, any extra irradiation does not increase the concentration of the peroxy radical. Hence, the ratio of E_1' centre with peroxy radical has been chosen for plotting variation with respect to time of irradiation. In case of grey quartz from SG-related vein (free from tungsten), there is an increase in the intensity ratio of the two resonance lines with increasing dosage of gamma irradiation. On the contrary, in case of quartz from W-mineralized vein of Motiya prospect as well as milky-white quartz from a vein intruding GG, there is a decrease in the intensity ratio of the two resonance lines with increasing dosage of gamma radiation.

From these EPR characteristics, we infer that diamagnetic W^{6+} ions present in quartz (P-49) from tungsten-mineralized quartz vein are converted to paramagnetic W^{5+} ion on gamma radiation. Interaction of these paramagnetic W^{5+} ions with free radicals in the E_1' centre has decreased the peak intensity corresponding to the E_1' centre, with increasing dosage of gamma radiation. Similarity in the EPR spectra of quartz from tungsten prospect (P-49) and the one from a quartz vein intruding into the Govindgarh granite (GG-227), shows that the latter belongs to the same category as the former. In the case of tungsten-free quartz sample (SG-137), with increasing dosage of gamma radiation there is an increase in peak intensity corresponding to the E_1' centre, due to development of more of these centres on gamma radiation. As a result of these contrasting trends, the intensity ratio of the two resonance lines (cor-

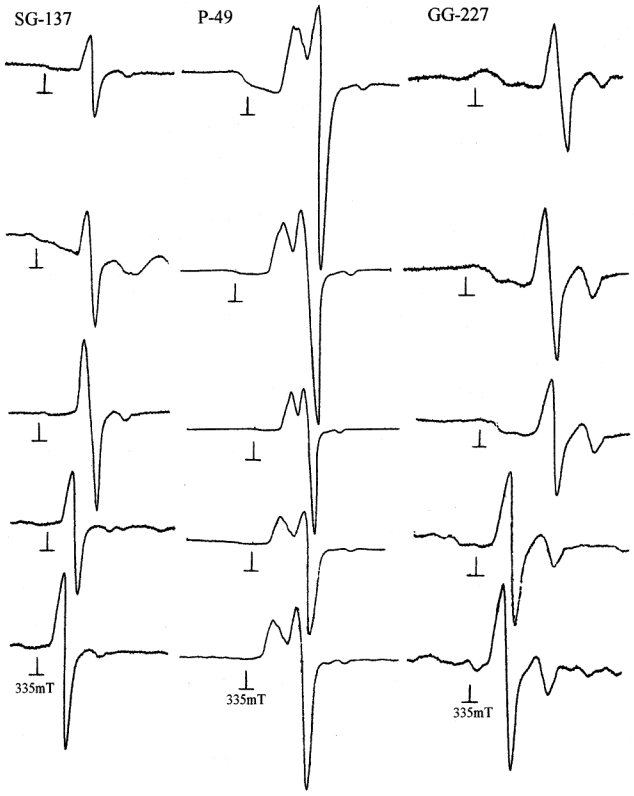

Figure 3. EPR spectra of three types of quartz samples after gamma irradiation, close to magnetic field strength of 335 mT. Five spectra from top to bottom in each column correspond to subset of each sample irradiated for 1, 2, 4, 6 and 8 h.

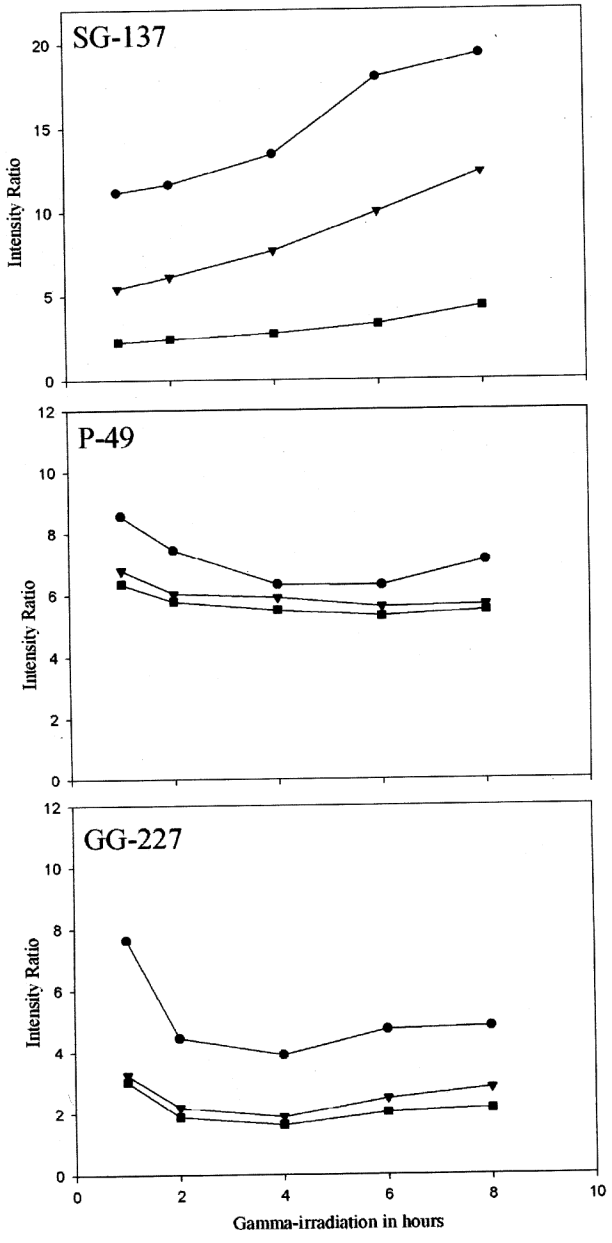

Figure 4. Irradiation time vs intensity ratio of resonance lines in EPR spectra of three types of quartz samples. Irradiation of 1, 2, 4, 6 and 8 h corresponds to 58, 116, 232, 348 and 464 krad respectively. Circle, Natural sample; triangle, Sample leached with HCl + HNO_3; square, Sample leached with HCl + HNO_3 + HF.

responding to the E_1' centre and peroxy radical) decreases in W-bearing quartz and increases in W-free quartz. However, in the case of P-49, a small increase in the ratio of intensities is noticed after 6 h of irradiation in only one sample. On the other hand, in case of GG-227, increase in intensity ratio was noticed between 4 and 6 h which then stabilized. A close look at the ratio of intensities indicates that the changes in P-49 and GG-227 are relatively small compared to those noticed in SG-137 and can be considered to be within experimental limits.

It is well known that the formation of various defects in quartz depends not only on the duration and temperature of irradiation, but also on other impurities present in quartz[4]. As the selected samples differ mainly in their concentration of W, the results have been explained by considering a possible mechanism involving W only. In addition, W^{5+} being a d^1 system, will give a single line around $g \sim 2$ and hyperfine structure will not be seen because of low abundance of ^{183}W (abundance = 14.3%)[13]. Except the above inference, we do not have any further evidence for the proposed mechanism. Further work is in progress in this direction.

In conclusion, the present preliminary study has demonstrated that it is possible to detect the association of W in quartz veins from EPR spectra of quartz samples irradiated to different dosages of gamma radiation. In addition, it is also suggested that even when W is below detection limits by normal techniques of chemical analysis, EPR provides a method of distinguishing the presence of W in quartz. Besides the usefulness of EPR technique to identify presence of W in quartz, the present article also attempts to prove that the EPR response is indeed due to presence of W. The current investigation highlights that the EPR technique can be used in conjunction with other geological and geochemical techniques for exploration of vein-type tungsten deposits.

1. Barnes, J. W., *Ores and Minerals: Introducing Economic Geology*, Wiley, New York, 1995, p. 181.
2. Wilson, T. M., Weil, J. A. and Sambasiva Rao, P., Electronic structure of the interstitial lithium-associated electron trap in crystalline quartz. *Phys. Rev. B*, 1986, **34**, 6053–6055.
3. Fowler, W. B., Sambasiva Rao, P., Weil, J. A. and Wilson, T. M., P substituted for Si in alpha-quartz: Defect structure and properties. *Bull. Am. Phys. Soc.*, 1987, **32**, 870.
4. Weil, J. A., A review of electron spin spectroscopy and its application to the study of paramagnetic defects in crystalline quartz. *Phys. Chem. Miner.*, 1984, **10**, 149–165.
5. Nuttall, R. H. D. and Weil, J. A., The magnetic properties of the oxygen-hole aluminum centres in crystalline SiO_2. I. $[AlO_4]^0$. *Can. J. Phys.*, 1981, **59**, 1696–1708.
6. Nuttall, R. H. D. and Weil, J. A., The magnetic properties of the oxygen-hole aluminum centers in crystalline SiO_2. II. $[AlO_4/H^+]^+$ and $[AlO_4/Li^+]^+$. *Can. J. Phys.*, 1981, **59**, 1709–1718.
7. Nuttall, R. H. D. and Weil, J. A., The magnetic properties of the oxygen-hole aluminum centers in crystalline SiO_2. III. $[AlO_4]^+$. *Can. J. Phys.*, 1981, **59**, 1886–1892.
8. Sambasiva Rao, P., Weil, J. A. and Williams, J. A. S., EPR investigations of carbonaceous natural quartz single crystals. *Can. Mineral.*, 1989, **27**, 219–224.
9. Motoji I., *New Applications of Electron Spin Resonance: Dating, Dosimetry and Microscopy*, World Scientific, Singapore, 1993, p. 500.
10. Jain, S. S. and Bhattacharjee, J., A note on the wolframite prospects associated with the Sewariya granite pluton, Rajasthan. *Indian Miner.*, 1992, **46**, 159–164.
11. Bhattacharjee, J., Fareeduddin and Jain, S. S., Tectonic setting, petrochemistry and tungsten metallogeny of the Sewariya granite in the South Delhi Fold Belt, Rajasthan. *J. Geol. Soc. India*, 1993, **42**, 3–16.
12. Pandian, M. S. and Dutta, S. K., Leucogranite magmatism in Sewariya–Govindgarh areas of Rajasthan and its relevance to tungsten mineralization. *J. Geol. Soc. India*, 2000, **55**, 289–295.
13. Rao, P. S. and Weil, J. A., EPR/ENDOR frequency Table, Bruker Almanac, 1997, p. 31–35.

ACKNOWLEDGEMENTS. The work was funded by a DST project to M.S.P. P.S.R. thanks Council of Scientific and Industrial Research, New Delhi for financial assistance. We thank the Head, Radiological Safety Division, IGCAR, Kalpakkam, for permission to use the Gamma Chamber. Constructive comments from the reviewers helped in improving the manuscript.

Received 29 July 2004; revised accepted 14 September 2005